Published in final edited form as:
Brain Res. 2007 September 7; 1168: 46–59.

AN EVOLVING CELLULAR PATHOLOGY OCCURS IN DORSAL ROOT GANGLIA, PERIPHERAL NERVE AND SPINAL CORD FOLLOWING INTRAVENOUS ADMINISTRATION OF PACLITAXEL IN THE RAT

Christopher M. Peters[1], **Juan Miguel Jimenez-Andrade**[1], **Michael A. Kuskowski**[5], **Joseph R. Ghilardi**[5], and **Patrick W. Mantyh**[1,2,3,4,5]

1*Department of Diagnostic & Biological Sciences, University of Minnesota, Minneapolis, MN 55455, USA*

2*Department of Neuroscience, University of Minnesota, Minneapolis, MN 55455, USA*

3*Department of Psychiatry, University of Minnesota, Minneapolis, MN 55455, USA*

4*Cancer Center, University of Minnesota, Minneapolis, MN 55455, USA*

5*Research Service, VA Medical Center, Minneapolis, MN 55417, USA*

6*GRECC, VA Medical Center, Minneapolis, MN 55417, USA*

Abstract

Paclitaxel (Taxol®) is a frontline antineoplastic agent used to treat a variety of solid tumors including breast, ovarian, or lung cancer. The major dose limiting side effect of paclitaxel is a peripheral sensory neuropathy that can last days to a lifetime. To begin to understand the cellular events that contribute to this neuropathy, we examined a marker of cell injury/regeneration (activating transcription factor 3; ATF3), macrophage hyperplasia/hypertrophy; satellite cell hypertrophy in the dorsal root ganglion (DRG) and sciatic nerve as well as astrocyte and microglial activation within the spinal cord at 1, 4, 6 and 10 days following intravenous infusion of therapeutically relevant doses of paclitaxel. At day 1 post-infusion there was an up-regulation of ATF3 in a subpopulation of large and small DRG neurons and this up-regulation was present through day 10. In contrast, hypertrophy of DRG satellite cells, hypertrophy and hyperplasia of CD68+ macrophages in the DRG and sciatic nerve, ATF3 expression in S100β+ Schwann cells and increased expression of the microglial marker (CD11b) and the astrocyte marker glial fibrillary acidic protein in the spinal cord were not observed until day 6 post infusion. The present results demonstrate that using the time points and markers examined, DRG neurons show the first sign of injury which is followed days later by other neuropathological changes in the DRG, peripheral nerve and dorsal horn of the spinal cord. Understanding the cellular changes that generate and maintain this neuropathy may allow the development of mechanism-based therapies to attenuate or block this frequently painful and debilitating condition.

Corresponding author: Patrick W. Mantyh, Neurosystems Center, 18-208 Moos Tower, University of Minnesota, 515 Delaware Street SE, Minneapolis, MN 55455, Phone: (612) 626-0180, Fax: (612) 626-2565, e-mail: manty001@umn.edu.

1. Introduction

Administration of the chemotherapeutic agent paclitaxel can induce a dose dependent peripheral sensory neuropathy in a subset of patients receiving this therapy for breast, ovarian, and non-small cell lung cancer (Lee & Swain, 2006; Mielke et al., 2006). Following administration of paclitaxel patients may experience a range of positive sensory symptoms including spontaneous tingling, burning pain, joint and muscle pain (Postma et al., 1995; Quasthoff & Hartung, 2002; Dougherty et al., 2004) that often occurs in the distal extremities in a “glove and stocking” distribution. These symptoms may increase in severity and be accompanied by sensory deficits including numbness, loss of vibratory sensation, decreased deep tendon reflexes and decreased proprioceptive abilities (Rowinsky et al., 1993; Postma et al., 1995). In many patients these symptoms spontaneously resolve following discontinuation of therapy, while in others they may persist for weeks to a lifetime (Pignata et al., 2006). Despite the widespread incidence of paclitaxel induced peripheral neuropathy (PIPN) and increasing use of paclitaxel in the treatment of various tumors (Giordano et al., 2006), there is currently no accepted standard of care to prevent/treat the pain or sensory dysfunction associated with this condition. The lack of standard treatment strategies is in part due to a lack of information regarding the cellular mechanisms responsible for the development of PIPN.

Recently, using a previously characterized model of PIPN (Cliffer et al., 1998), we demonstrated pathological features in the dorsal root ganglia (DRG) and sciatic nerve ten days following intravenous administration of paclitaxel in rats (Peters et al., 2007). This cellular pathology was accompanied by behavioral changes indicative of a sensory neuropathy including cold and mechanical allodynia as well as behavioral deficits in coordination (Peters et al., 2007). Examination of sensory ganglia at multiple levels of the neuroaxis revealed that the cellular pathology occurred in a length dependent manner (Jimenez-Andrade et al., 2006) similar to the pattern of symptoms observed in patients treated with taxanes. What remains unknown is the time course of the evolution of cellular events that occur following intravenous paclitaxel administration. In the current study, we examined the time course of changes in markers of cell injury/regeneration (ATF3), activation of satellite cells (GFAP), macrophage hypertrophy and hyperplasia (CD68) and microglial and astrocyte activation/hypertrophy (CD11b and GFAP, respectively) within the DRG, sciatic nerve, and spinal cord following intravenous administration of paclitaxel in the rat.

2. Results

2.1 Time course of neuronal and non-neuronal ATF3 expression in the DRG of paclitaxel-treated rats

In the current study, we examined immunohistochemically the levels of activating transcription factor 3 (ATF3) in the DRG of rats that received intravenous paclitaxel or vehicle. We administered two infusions of paclitaxel at a dose of 18 mg/kg (day 0 and day 3; 36 mg/kg cumulative dose). We examined ATF3 expression in lumbar DRG (L4) at days 1, 4, 6 and 10 following the first infusion. The percentage of ATF3-IR neuronal profiles significantly increased in paclitaxel-treated rats compared to vehicle-treated rats at all time points examined (Figs. 1B-E). The percentage of total ATF3-IR sensory neurons in L4 DRG following i.v. paclitaxel was 1.1 ± 0.1 %, 27.6 ± 3.4 %, 25.7± 5.7 %, and 5.1± % at day 1, 4, 6, and 10, respectively ($n \geq 5$ each time point). The percentage of ATF3-IR neuronal profiles in vehicle-treated rats was minimal at each time point (Fig. 1B, 0.2 ± 0.1%, 0.2 ± 0.1%, 0.2 ± 0.1%, and 0.3± 0.1% on day 1, 4, 6, and 10, respectively; n=4 each time point) and not significantly different than levels in naïve rats (data not shown). Comparison between time points demonstrated that the percentage of total sensory neurons within L4 DRG expressing ATF3 was significantly greater at day 4 and day 6 compared to day 1 and day 10 after paclitaxel infusion (Table 1, $p<0.05$). In pilot experiments we examined expression of additional markers

of cell injury and apoptosis in DRG of paclitaxel treated rats at day 4, 6 and 10 post infusion including terminal dUTP nick-end labeling (TUNEL) and immunohistochemistry with an antibody for active caspase 3. No evidence of TUNEL staining or active caspase 3 immunoreactivity was present at any of the time points examined (data not shown).

Paclitaxel treatment also increased the ATF3 expression in non-neuronal cell populations at day 10 (Fig. 1E, arrowhead). Non-neuronal ATF3 expression within the DRG of paclitaxel-treated rats occurred in satellite cells which were identified based on the presence of GFAP (Fig. 1F). The majority of ATF3-IR satellite cells were located in distinct clusters (>8) of nuclei (Fig. 1E, arrowhead). The number of ATF3-IR satellite cell clusters present in paclitaxel-treated rats was significantly greater than in vehicle-treated rats (27 ± 4 ATF3-IR satellite cell clusters/four L4 DRG sections paclitaxel-treated rats compared to 0 ± 0 ATF3-IR satellite cell clusters/four L4 DRG sections vehicle-treated rats) at day 10. ATF3-IR satellite cells clusters were not observed in DRG of paclitaxel or vehicle-treated rats prior to day 10.

2.2 Cell size distribution of neuronal ATF3 expression in DRG of paclitaxel-treated rats

In order to characterize the subset of sensory neurons that express ATF3 at various time points following paclitaxel treatment, we examined the percentage of sensory neurons that expressed ATF3 within specific size classes in paclitaxel-treated rats. The neuronal cell soma area was determined in DRG of paclitaxel-treated rats for a minimum of 700 neuronal profiles per time point. Previously, we observed that large > medium > small diameter sensory neurons expressed ATF3 ten days following paclitaxel administration (Peters et al., 2007). This pattern was also observed in the current study at earlier time points including days 4 and 6 post initial infusion. The percentage of small sized sensory neurons that expressed ATF3 at various time points was 1.3 ± 0.3 % (Day 1); 8.7 ± 2.1% (Day 4); 4.5 ± 1.7 % (Day 6) and 2.1 ± 0.7 % (Day 10). The percentage of medium sensory neurons that expressed ATF3 at various time points was 1.9±0.7 % (Day 1); 40.2±5.7 % (Day 4); 24.1 ± 8.6 % (Day 6) and 11.6 ±3.0 % (Day 10). The percentage of large sensory neurons that expressed ATF3 at various time points was 3.6 ± 0.4 % (Day 1), 58.4 ± 5.7 % (Day 4); 63.0 ± 12.0 % (Day 6) and 26.7 ± 7.5 % (Day 10).

2.3 Time course of morphological alterations (GFAP-IR) in satellite cells and neural inflammation (CD68-IR) in the DRG of paclitaxel-treated rats

We measured changes in the immunofluorescence (IF) levels of the intermediate filament glial fibrillary acidic protein (GFAP) in satellite cells of rats. In normal rats, low levels of GFAP are present in DRG satellite cells (Jessen et al., 1984). Immunofluorescence levels of GFAP in L4 ganglia were increased in paclitaxel-treated rats compared to vehicle-treated rats from day 6 (7141 ± 1798 % paclitaxel-treated rats versus 100 ± 53 % vehicle-treated rats) through day 10 (5532 ± 603 % paclitaxel treated rats versus 100 ± 7 % vehicle-treated rats) (Table 1, Fig. 2). Satellite cells in paclitaxel treated rats exhibiting increased GFAP-IR were present around small, medium, and large sized sensory neurons and possessed a more hypertrophic appearance compared to satellite cells in vehicle-treated rats (Figs. 2D). There were no significant differences in GFAP IF levels between paclitaxel-treated rats compared to vehicle-treated rats at day 1 or 4 post infusion (data not shown).

We identified macrophage activation using an antibody against CD68, a lysosomal membrane protein that is primarily found in active phagocytic macrophages (Damoiseaux et al 1994). We quantified the number of CD68-IR macrophages in L4 DRG of vehicle and paclitaxel-treated rats at 1, 4, 6, and 10 days post initial infusion. The number of macrophages was significantly increased in paclitaxel-treated compared to vehicle-treated rats from day 6 (400 ± 53 CD68-IR macrophages/mm^2 paclitaxel-treated rats versus 137 ± 19 CD68-IR macrophages/mm^2 vehicle-treated rats) through day 10 (892 ± 56 CD68-IR macrophages/mm^2 paclitaxel-treated rats versus 72 ± 13 CD68-IR macrophages/mm^2 vehicle-treated rats) (Table 1, Fig. 3). There

was no significant difference in number of CD68-IR macrophages between paclitaxel-treated rats compared to vehicle-treated rats at day 1 or 4 post infusion (data not shown). Morphologically CD68-IR macrophages in paclitaxel-treated rats had a greater size and more cytoplasmic CD68 labeling than macrophage in vehicle-treated rats at day 6 and 10 (Table 1, Fig. 3D) suggesting that they possess a more active phenotype.

2.4 Cellular changes in the sciatic nerve following intravenous paclitaxel

Schwann cell activation, demyelination, and macrophage activation commonly accompany injury to the peripheral nerve as a result of axonal degeneration. Anatomically, non-myelinating Schwann cells are associated with axons of small diameter sensory neurons and are identified based on the expression of the intermediate filament GFAP (Jessen & Mirsky, 1984). Myelinating Schwann cells are associated with axons of medium and large diameter sensory neurons and are identified based on expression of S100β protein which is localized to the outermost parts of the myelin sheath (Stefansson et al., 1982). We examined sections of sciatic nerve obtained at mid-thigh level for expression of ATF3. ATF3-IR was present predominantly in S100β-IR Schwann cells within the endoneurium of paclitaxel- treated rats (Fig. 4C, E). The number of ATF3-IR Schwann cells was significantly greater in the sciatic nerve of paclitaxel-treated versus vehicle- treated rats at day 6 (46 ± 22 ATF3-IR Schwann cells/mm^2 paclitaxel-treated rats versus 0.3 ± 0.3 ATF3-IR Schwann cells/mm^2 vehicle-treated rats) through day 10 post initial infusion (400 ± 27 ATF3-IR Schwann cells/mm^2 paclitaxel-treated rats versus 0.5 ± 0.5 ATF3-IR Schwann cells/mm^2 vehicle-treated rats) (Table 1, Fig. 4A,C,E). There were only occasional ATF3-IR Schwann cells in paclitaxel-treated or vehicle-treated rats at day 1 or 4 post initial infusion (data not shown).

We also examined GFAP levels in non-myelinating Schwann cells in order to determine if similar alterations observed in DRG satellite cells occurred in the peripheral nerve. There was no significant difference in IF levels of GFAP between paclitaxel or vehicle-treated rats at any of the time points examined (data not shown). Additionally, ATF3-IR did not colocalize with GFAP-IR nonmyelinating Schwann cells at the time points examined (data not shown).

Additionally, the number of CD68-IR macrophages in the sciatic nerve was significantly greater in paclitaxel compared to vehicle-treated rats at day 10 (324 ± 2 CD68-IR macrophages/mm^2 paclitaxel-treated rats versus 39 ± 10 CD68-IR macrophages/mm^2 vehicle-treated rats) (Table 1, Fig. 4B, D and F). There was no significant difference in number of CD68-IR macrophages in the sciatic nerve between paclitaxel-treated rats compared to vehicle treated rats at day 1, 4, or 6 (data not shown). Spatially, CD68-IR profiles were present throughout the endoneurium. In contrast, during earlier time points and in vehicle-treated rats CD68-IR cellular profiles were sparse and were primarily associated with blood vessels within the endoneurium (data not shown).

2.5 Microglial and astrocyte activation occurs within the spinal cord following intravenous paclitaxel

To examine whether neurochemical reorganization in the spinal cord occurs following intravenous paclitaxel administration, we examined lumbar spinal cord sections using immunohistochemistry with antibodies to CD11b and GFAP to label microglia and astrocytes, respectively. Microglial activation was measured as an increase in the intensity and area of CD11b-IR in the spinal cord of treated rats. Levels of CD11b-IR in superficial laminae (I-II) of paclitaxel-treated rats were not significantly greater than vehicle levels (Table 1). Within deep laminae (III-VI), IF levels of CD11b were significantly greater in paclitaxel-treated rats compared to vehicle-treated rats at day 6 (180 ± 46% laminae III-VI paclitaxel-treated rats versus 100 ± 25% laminae III-VI vehicle-treated rats) and day 10 (348 ± 58% laminae III-VI paclitaxel-treated rats versus 100 ± 36% laminae III-VI vehicle-treated rats. There was no

significant increase in CD11b IF levels in deep lamina between paclitaxel and vehicle-treated rats at earlier time points (Table 1). The density of microglia in vehicle-treated rats was uniform throughout the gray matter of the spinal cord and similar to levels in age matched naïve animals (Table 1, Fig. 5A, C). Microglia in paclitaxel-treated rats were more densely distributed within laminae III-VI and possessed a hypertrophied appearance compared to microglia in vehicle-treated rats (Figure 5B, D) which possessed a highly ramified morphology simlar to microglia in naïve rats.

Astrocyte activation was measured as an increase in the intensity and area of GFAP IR in the spinal cord of treated rats (Garrison et al., 1994). levels of GFAP-IR in superficial laminae of paclitaxel-treated rats were significantly greater than vehicle levels at day 6 (173 ± 27% laminae I-II paclitaxel-treated rat versus 100 ± 3% laminae I-II vehicle-treated rats) and day 10 (145 ± 21% laminae I-II paclitaxel-treated rat versus 100 ± 3% laminae I-II vehicle-treated rats)(Fig. 6, Table 1). There was no increase in GFAP IF levels in superficial lamina between paclitaxel and vehicle-treated rats at earlier time points (Table 1). Within deep laminae (III-VI), IF levels of GFAP were increased in paclitaxel-treated rats compared to vehicle-treated rats at day 6 (163 ± 38% laminae III-VI paclitaxel-treated rat versus 100 ± 3% laminae III-VI vehicle-treated rats) and day 10 (147 ± 33% laminae III-VI paclitaxel-treated rat versus 100 ± 3% laminae III-VI vehicle-treated rats). Astrocytes within the dorsal horn of the spinal cord of paclitaxel treated rats possessed a more hypertrophied in appearance compared to astrocytes in vehicle-treated rats (Fig. 6).

3. Discussion

3.1 Impact of intravenous paclitaxel on sensory neurons in the DRG

PIPN is a continuing challenge in the treatment of cancer as it can have a significant impact on cancer patient's quality of life and survivorship (Mantyh, 2006). Despite the widespread incidence of this neuropathy, the cellular mechanisms responsible for its development are largely unknown. In the present study, the up-regulation of ATF3 by a subset of small, medium and large sensory neurons was the first cellular marker of those we examined to show a change following intravenous infusion of paclitaxel. The up-regulation of ATF3 in DRG neurons was first noted at day 1 following the initial intravenous infusion and this increased expression was still present at day 10 post-infusion (the latest time point examined). Previous studies have shown that ATF3 is induced by stress stimuli and cellular damage and may have a survival/regenerative function in sensory neurons (Seijffers et al., 2006) Following axotomy of sensory nerve fibers within the sciatic nerve (Tsujino et al., 2000), spinal nerves (Wang et al., 2003), or distal branches of the sciatic nerve (Tsuzuki et al., 2001) in the rat, ATF3 is up-regulated in neuronal cell bodies within 24 hours and this de novo expression can be maintained for weeks (Tsujino et al., 2000; Tsuzuki et al., 2001; Shortland et al., 2006). Upregulation of ATF3 in the DRG of axotomized nerves is prevented by the exogenous administration of nerve growth factor (Averill et al., 2004) and glial cell derived nerve growth factor (Wang et al., 2003). From these studies, it has been suggested that ATF3 expression is induced as a result of decreased availability of target derived growth factors. This data, as well as data showing that paclitaxel acts by enhancing tubulin polymerization suggests that paclitaxel induced ATF3 expression in sensory neurons may in part be due to the ability of paclitaxel to bind to microtubules leading to impaired axonal transport of growth factors and molecules required for normal nerve function.

Recent reports suggest that paclitaxel may also have direct toxic effects on sensory neuron cell bodies (Cavaletti et al., 2000; Scuteri et al., 2006). In the current study, we observed a significant decrease in the percentage of sensory neurons expressing ATF3 between day 6 and day 10 post infusion (26 to 5% total L4 DRG). This decreased level of neuronal ATF3 may occur as a result of downregulation of ATF3 and/or due to the death of a subset of ATF3

expressing neurons. Interestingly, the decrease in neuronal ATF3 expression observed at day 10 post-infusion coincided with an increase in clusters of ATF3 expressing satellite cells. These clusters of ATF3-IR satellite cells are similar in appearance to nodules of Nageotte which are compact groups of aggregating satellite cells that have been described to form in response to degeneration or loss of sensory neurons within the DRG (Thomas et al., 1992). This observation suggests that in the current rat model as early as ten days post-infusion paclitaxel may induce a permanent and irreversible loss of a subset of primary afferent neurons. In support of this claim, a previous study that examined the distribution of paclitaxel in the rat nervous system reported that approximately seven fold higher levels of paclitaxel accumulate in the DRG compared to the sciatic nerve (Cavaletti et al., 2000). Paclitaxel applied to postmitotic DRG explants from E15 mice induced necrotic cell death (Scuteri et al., 2006) in sensory neurons without the appearance of cellular hallmarks of apoptosis. Administration of calpain inhibitors, which inactivate cysteine proteases that mediate cellular degradation associated with necrotic cell death, reduced axonal degeneration following intravenous administration of paclitaxel in mice (Wang et al., 2004). Collectively these studies suggest that paclitaxel may elicit its neurotoxic effects on sensory neurons via a necrotic mechanism. These data fit with human post mortem studies that report a higher incidence of nodules of Nagoette in the DRG of patients with cisplatin induced neuropathy and clinical studies that report severe axonal degeneration in sural nerve biopsies of patients with taxane induced neuropathy (Sahenk et al., 1994; Fazio et al., 1999). Understanding the precise mechanism by which paclitaxel induces sensory neuron cell death remains an open question.

3.2 Cellular alterations in satellite cells, macrophages and Schwann cells

In normal sensory ganglia, each neuronal cell body is surrounded by satellite cells associated with a basal lamina. Functionally, satellite cells are responsible for maintaining the homeostasis of sensory neurons by regulating extracellular ion and nutrient levels within the DRG (For review see (Hanani, 2005). Following sciatic nerve axotomy in rats, satellite cells have been shown to undergo morphological changes (Woodham et al., 1989; Stephenson & Byers, 1995), proliferate (Shinder & Devor, 1994) and upregulate a variety of growth factors (Hammarberg et al., 1996; Zhou et al., 1999). Additionally, hypertrophy and up-regulation of GFAP in satellite cells has been observed following mechanical injury to the peripheral terminals of sensory neurons that innervate the teeth whose cell bodies are housed within trigeminal ganglia (Stephenson & Byers, 1995). In the current study, there was a significant hypertrophy of satellite cells at day six and ten post-infusion as evidenced by an increase in GFAP-IR. It has been suggested that paclitaxel-induced neuropathy may involve injury or alterations in another supporting cell, the Schwann cell, which may contribute to demyelination and axonal degeneration of peripheral nerve fibers (Cavaletti et al., 1995). In the current study, we observed *de novo* ATF3 expression in myelinating (S100β-IR) Schwann cells in the sciatic nerve at day six post-infusion. Interestingly, the Schwann cells showing ATF-3 up-regulation tended to be arranged in a linear fashion as if a group of Schwann cells that ensheath the same injured axon were all expressing ATF3. These data are consistent with previous morphological and ultrastructural studies which showed pronounced degenerative changes in Schwann cells and axons located within the sciatic nerve and dorsal roots, but not ventral roots of rats that received intravenous infusion of paclitaxel (Cliffer et al., 1998; Persohn et al., 2005).

In the present study six days following initial infusion of paclitaxel there was a significant hypertrophy and hyperplasia of macrophages in both the DRG and sciatic nerve. Previous studies following axotomy of primary afferent sensory nerves has been shown to promote the activation and migration of macrophages within the peripheral nerve (Myers et al., 1996; Tofaris et al., 2002; Abbadie et al., 2003) and associated DRG (Hu & McLachlan, 2002). The increased number of macrophages observed may be due to proliferation of resident macrophages or due to infiltration of hematogeneous macrophages into the DRG (Mueller et

al., 2003). Functionally, macrophage activation within the DRG and peripheral nerve following peripheral nerve injury is known to help remove degenerating neuronal debris and myelin as well as contribute to subsequent regeneration (Lu and Richardson 1993, Perry and Brown 1992, Hu and McLachlan 2002). Recently, it has been recognized that inflammatory responses in the DRG may also contribute to the development pathological pain states (Cui et al., 2000; Xie et al., 2006) through the release of a variety of proinflammatory factors which are capable of sensitizing primary afferent neurons whose cell bodies are housed in the DRG (Taniuchi et al., 1986; Lindholm et al., 1987; Meyer et al., 1992; Hammarberg et al., 1996; Ma & Eisenach, 2002, 2003).

3.3. Markers indicative of microglia and astrocyte activation are altered in the spinal cord of paclitaxel-treated rats

It is widely recognized that spinal glial activation following peripheral nerve injury or inflammation may be involved in altered spinal processing of sensory information (Kajander et al., 1990; Nichols et al., 1997; Aldskogius et al., 1999; Watkins et al., 2001) and the development of tactile allodynia (Jin et al., 2003; Tsuda et al., 2003). In the current study, an increase in the levels of CD11b-IR microglia and GFAP-IR astrocytes was first observed at day six days post-infusion in the dorsal horn of the spinal cord of paclitaxel-treated rats. Paclitaxel has a limited ability to cross the blood brain barrier in that the plasma/cerebrospinal fluid ratio of paclitaxel is greater than 500:1(Glantz et al., 1995). Therefore, the present data suggest that this glial activation occurs as a result of degeneration of central terminals of injured primary afferent fibers (Kapadia & LaMotte, 1987; Aldskogius et al., 1999) or possibly due to the spinal release of factors from injured sensory neurons (Tsuda et al., 2005) rather than due to a direct effect of paclitaxel on spinal cord neurons. Interestingly, significant microglial and astrocyte activation occurred in different regions of the spinal cord of paclitaxel treated rats suggesting a different glial response following injury to small vs. large sensory fibers. Thus, there was only a significant increase in the microglial marker CD11b in laminae III-VI which is the area of the dorsal horn where large myelinated sensory fibers that primarily innervate muscle and joints terminate (Todd & Koerber, 2006). In contrast, the greatest increase in the astrocyte marker GFAP-IR occurred in laminae I & II which is where the central terminals of most small C-fibers terminate. These data suggest that both A and C fibers are impacted by paclitaxel but the extent and severity of injury may vary between different populations of sensory neurons.

Summary—In the present study, we demonstrate that paclitaxel induces injury of sensory neurons, morphological and biochemical alterations in DRG satellite cells, hyperplasia/hypertrophy of macrophages in the peripheral nervous system, and increased microglial and astrocyte activation with the spinal cord. Collectively, these cellular alterations may contribute to the sensory dysfunction and pain that accompanies the development of PIPN. Preemptive or post-treatment strategies that target one or more of these pathological events may have the potential to prevent/treat the development of this neuropathy.

4. Experimental Procedure

4.1 Animals and drugs

All procedures were approved by the Institutional Animal Care and Use Committee at the University of Minnesota. Adult male Sprague Dawley rats (250-275 g, Harlan, Indianapolis, IN) were used in the present study. Paclitaxel was formulated by dissolving paclitaxel (Eton Bioscience, San Diego, CA) in Cremophor EL and dehydrated ethanol (1:1) to make a stock solution of 12 mg/ml. Prior to administration, the paclitaxel solution was further diluted with sterile saline (1:3). The paclitaxel solution or equivalent volume of vehicle (Cremophor EL/ethanol/saline, 1:1:6) was slowly injected intravenously into the tail vein at a dose of 18 mg/

kg day 0 and day 3; 36 mg/kg cumulative dose (Cliffer et al., 1998) while rats were under 3% isofluorane anesthesia. An intravenous route of administration was used because this is the most common route of administration for cancer patients receiving paclitaxel (Mielke et al., 2006). The dosing regimen used for this study was shown by Cliffer et al. to induce a sensory neuropathy based on physiological and histological endpoints with minimal effects on the general health of the animals (Cliffer et al., 1998). Based on FDA recommended conversion factors for preclinical oncology studies, the cumulative paclitaxel dose of 36 mg/kg administered to rats is equivalent to a dose of 216 mg/m^2 in humans (www.fda.gov/cder/cancer/animalframe.htm) which falls within the range of therapeutic doses administered to cancer patients (Lee & Swain, 2006; Mielke et al., 2006).

4.2 Immunohistochemistry

One, four, six and ten days following the initial paclitaxel ($n \geq 5$ in each time point) or vehicle administration ($n \geq 4$ in each time point), animals were sacrificed and the tissue was processed for immunohistochemical analysis as previously described (Peters et al., 2005). Briefly, rats were perfused intracardially with 200 ml of 0.1 M phosphate buffered saline (PBS) followed by 200 ml of 4% formaldehyde/12.5% picric acid solution in 0.1 M PBS. The DRG (L4), sciatic nerves, and lumbar spinal cord were removed, post-fixed for 4 hours in the perfusion fixative, and cryoprotected for 24 hours in 30% sucrose in 0.1 M PBS all at 4°C. We focused our examination on the L4 DRG level based on a previous study that demonstrated the most severe pathology following i.v. paclitaxel was present in lumbar (L4) compared to trigeminal and thoracic ganglia (Jimenez-Andrade et al., 2006). Additionally, anatomically a significant percentage of cell bodies of sensory neurons that innervate the rat hindlimb muscle and glabrous skin are present at the L4 level (Molander C, 1987; Baron et al., 1988). Additionally, in preliminary experiments the levels of ATF3 expression in L4 DRG of paclitaxel treated rats ten days following paclitaxel administration were not statistically different compared to values in L3 and L5 DRG. Serial frozen sections of L4 DRG or sciatic nerve were cut at 15 μm on a cryostat and mounted onto gelatin-coated slides for immunohistochemical analysis. The DRG and sciatic nerve sectioned tissue was incubated 60 minutes at room temperature (RT) in a blocking solution of 3% normal donkey serum in PBS with 0.3% Triton-X100. Sections were incubated overnight at RT with antibodies against activating transcription factor 3 (rabbit anti-ATF3, 1:500, Santa Cruz Biotechnology, Santa Cruz, CA), glial fibrillary acidic protein (rabbit anti-GFAP, 1:1000, Dako, Copenhagen, Denmark) or for double labeling with ATF3 (goat anti-GFAP, 1:500, Santa Cruz Biotechnology, Santa Cruz, CA), CD68 (mouse anti-CD68, clone ED1, 1:5000, Serotec, Raleigh, NC) which labels activated macrophages, neuronal nuclei antigen (mouse anti-NeuN, 1:150, Chemicon, Temecula, CA), and the calcium binding protein S100β (1;1000, Sigma, St. Louis. MO) which labels myelinating Schwann cells. Lumbar spinal cord sections were labeled with antibodies against CD11b (mouse anti-rat CD11b, clone OX42, Serotec Ltd.) which labels microglia and GFAP (rabbit anti-GFAP, 1:1000, Dako, Copenhagen, Denmark) which labels astrocytes. Sections were washed in PBS and incubated for three hours at RT with secondary antibodies conjugated to various fluorescent markers (Cy2 1:200, Cy3 1:600; Jackson ImmunoResearch, West Grove, PA). Finally, the sections were washed 3 × 10 minutes in PBS, mounted on gelatin-coated slides, dried, dehydrated via an alcohol gradient (70, 90 and 100%), cleared in xylene, and coverslipped with DPX. To confirm the specificity of the primary antibodies, controls included preabsorption with the corresponding synthetic peptide or omission of the primary antibody.

4.3 Quantification/ Image analysis

The number of ATF3 positive cellular profiles in L4 DRG was determined as previously reported (Peters et al., 2005). The cell size distribution of ATF3 in neuronal subsets was determined by measuring the soma area (Image Pro Plus v 3.0) of individual ATF3 and NeuN positive profiles in three paclitaxel-treated rats per each time point. Results are reported as the

percentage of labeled cells within each size population according to previously established size criteria (Obata et al., 2003) small (<600 μm^2), medium (600-1200 μm^2) and large (>1200 μm^2) neurons. The number of nodules of Nageotte was determined by counting the total number of clusters (> 8 adjacent nuclei) of ATF3-IR satellite cells in the entire area of a DRG section from a total of 4 sections per ganglion (Peters et al., 2007).

To assess satellite cell activation in the DRG, GFAP immunofluorescence (IF) levels were quantified (Peters et al., 2007). Satellite cells have been shown to increase the levels of GFAP expression as well as increase their size following peripheral nerve injury (Woodham et al., 1989; Shinder & Devor, 1994). Therefore both the immunofluorescence intensity as well as the area of the cell labeled were determined as a measure of satellite cell activation. Images from 3 randomly chosen regions (250 μm × 250 μm observation field) in each DRG section were digitized using an Olympus BX51 fluorescent microscope fitted with an Olympus DP70 digital CCD camera by an investigator blind to the treatment group of the animals. Only regions of the DRG that contained neuronal cell bodies rather than sensory axons were imaged. A minimum of four sections from each vehicle or paclitaxel treated rats were quantified. The integrated optical density (IOD) was determined using Image Pro Plus v 3.0. Integrated optical density is a previously used methodology (Garrison et al., 1994; Cameron et al., 1997) that is determined by averaging the intensity of fluorescence × area of labeling within a defined immunofluorescence intensity threshold. The intensity threshold was set to exclude nonspecific background fluorescence and applied to all sections analyzed. Results for each region were expressed as IOD/ total area sampled for the given section. Values from a minimum of four sections were averaged for each rat. To control for sample to sample variability in immunofluorescence measurements the mean IF values from paclitaxel-treated rats were expressed as percentage of vehicle-treated rat values sacrificed and processed at the same time point.

To determine the extent of neural inflammation within sensory ganglia and sciatic nerve following paclitaxel or vehicle treatment, we quantified the number of CD68-IR macrophages. The antibody to CD68 labels a lysosomal protein that is present in phagocytically active macrophage. Upregulation of CD68 indicates that cells are accumulating lysosomal vacuoles (Damoiseaux et al., 1994). Briefly, three regions (250 μm × 250 μm observation field) were randomly chosen within each DRG section and the number of CD68-IR cells was counted at X400 magnification. A minimum of four separate sections were assessed for each ganglion and the results were expressed as number of CD68-IR profiles/mm^2. Only CD68-IR cellular profiles that displayed visible nuclei as determined by counterstaining with DAPI were counted. The size of macrophages may also increase when they become phagocytically active. While we observed an increase in size of CD68-IR macrophages in DRG following paclitaxel administration, we did not quantify this change because CD68 expression within macrophages of control rats was minimal and was not present throughout the cytoplasm presumably due to low lysosomal vacuolization which did not allow for accurate assessment actual macrophage size. For quantifying the number of ATF3-IR and CD68-IR cells within the sciatic nerve the same manual counting system described above was used (Peters et al., 2007).

For analysis of immunofluorescence for CD11b and GFAP in the lumbar spinal, a minimum of least six randomly selected sections of the spinal cord were used from each animal. Images were captured on an Olympus BX51 fluorescent microscope fitted with an Olympus DP70 digital camera. The mean fluorescence intensity × area of positive staining (Integrated Optical Density, IOD) was determined within a defined fluorescence intensity threshold applied to all sections and analyzed using Image Pro Plus software. The IOD results were expressed per total sampled area within the given section. The IOD values for each section within an experimental animal were averaged. The IOD of spinal cord sections of paclitaxel-treated rats were expressed as percentage of vehicle-treated levels (100%) from rats sacrificed and processed at the same

time point. There were no statistically significant differences in immunofluorescence levels between vehicle-treated and age-matched naïve rats (data not shown).

4.4 Statistical Analysis

Wilcoxon matched-pair signed ranks tests were used to compare paclitaxel and vehicle responses in the same animals at each time point. To compare different neuron size groups at each sacrifice day, Friedman non-parametric repeated measures analysis of variance, followed by Wilcoxon two-group matched-pair tests between neuron size types were used. To compare relative neuronal ATF3 expression between sacrifice days (days 1, 4, 6 and 10) following paclitaxel treatment separate non-parametric analyses of variance (Kruskal-Wallis) were run followed by two-group day versus day comparisons (Mann-Whitney). Vehicle data was examined in the same fashion. Results were considered statistically significant at $P<0.05$.

Acknowledgements

This work was supported by National Institutes of Health grants (NS23970, NS048021) a Merit Review from the Veterans Administration and NIH Musculoskeletal Training grant T32 AR 050938-01.

References

Abbadie C, Lindia JA, Cumiskey AM, Peterson LB, Mudgett JS, Bayne EK, DeMartino JA, MacIntyre DE, Forrest MJ. Impaired neuropathic pain responses in mice lacking the chemokine receptor CCR2. Proc Natl Acad Sci U S A 2003;100:7947–7952. [PubMed: 12808141]

Aldskogius H, Liu L, Svensson M. Glial responses to synaptic damage and plasticity. J Neurosci Res 1999;58:33–41. [PubMed: 10491570]

Averill S, Michael GJ, Shortland PJ, Leavesley RC, King VR, Bradbury EJ, McMahon SB, Priestley JV. NGF and GDNF ameliorate the increase in ATF3 expression which occurs in dorsal root ganglion cells in response to peripheral nerve injury. Eur J Neurosci 2004;19:1437–1445. [PubMed: 15066140]

Baron R, Janig W, Kollmann W. Sympathetic and afferent somata projecting in hindlimb nerves and the anatomical organization of the lumbar sympathetic nervous system of the rat. J Comp Neurol 1988;275:460–468. [PubMed: 3225349]

Cameron AA, Cliffer KD, Dougherty PM, Garrison CJ, Willis WD, Carlton SM. Time course of degenerative and regenerative changes in the dorsal horn in a rat model of peripheral neuropathy. Journal of Comparative Neurology 1997;379:428–442. [PubMed: 9067834]

Cavaletti G, Cavalletti E, Oggioni N, Sottani C, Minoia C, D'Incalci M, Zucchetti M, Marmiroli P, Tredici G. Distribution of paclitaxel within the nervous system of the rat after repeated intravenous administration. Neurotoxicology 2000;21:389–393. [PubMed: 10894128]

Cavaletti G, Tredici G, Braga M, Tazzari S. Experimental peripheral neuropathy induced in adult rats by repeated intraperitoneal administration of taxol. Exp Neurol 1995;133:64–72. [PubMed: 7601264]

Cliffer KD, Siuciak JA, Carson SR, Radley HE, Park JS, Lewis DR, Zlotchenko E, Nguyen T, Garcia K, Tonra JR, Stambler N, Cedarbaum JM, Bodine SC, Lindsay RM, DiStefano PS. Physiological characterization of Taxol-induced large-fiber sensory neuropathy in the rat. Ann Neurol 1998;43:46–55. [PubMed: 9450768]

Cui JG, Holmin S, Mathiesen T, Meyerson BA, Linderoth B. Possible role of inflammatory mediators in tactile hypersensitivity in rat models of mononeuropathy. Pain 2000;88:239–248. [PubMed: 11068111]

Damoiseaux JG, Dopp EA, Calame W, Chao D, MacPherson GG, Dijkstra CD. Rat macrophage lysosomal membrane antigen recognized by monoclonal antibody ED1. Immunology 1994;83:140–147. [PubMed: 7821959]

Dougherty PM, Cata JP, Cordella JV, Burton A, Weng HR. Taxol-induced sensory disturbance is characterized by preferential impairment of myelinated fiber function in cancer patients. Pain 2004;109:132–142. [PubMed: 15082135]

Fazio R, Quattrini A, Bolognesi A, Bordogna G, Villa E, Previtali S, Canal N, Nemni R. Docetaxel neuropathy: a distal axonopathy. Acta Neuropathol (Berl) 1999;98:651–653. [PubMed: 10603043]

Garrison CJ, Dougherty PM, Carlton SM. GFAP expression in lumbar spinal cord of naive and neuropathic rats treated with MK-801. Exp Neurol 1994;129:237–243. [PubMed: 7957738]

Giordano SH, Duan Z, Kuo YF, Hortobagyi GN, Freeman J, Goodwin JS. Impact of a scientific presentation on community treatment patterns for primary breast cancer. J Natl Cancer Inst 2006;98:382–388. [PubMed: 16537830]

Glantz MJ, Choy H, Kearns CM, Mills PC, Wahlberg LU, Zuhowski EG, Calabresi P, Egorin MJ. Paclitaxel disposition in plasma and central nervous systems of humans and rats with brain tumors. J Natl Cancer Inst 1995;87:1077–1081. [PubMed: 7616600]

Hammarberg H, Piehl F, Cullheim S, Fjell J, Hokfelt T, Fried K. GDNF mRNA in Schwann cells and DRG satellite cells after chronic sciatic nerve injury. Neuroreport 1996;7:857–860. [PubMed: 8724660]

Hanani M. Satellite glial cells in sensory ganglia: from form to function. Brain Res Brain Res Rev 2005;48:457–476. [PubMed: 15914252]

Hu P, McLachlan EM. Macrophage and lymphocyte invasion of dorsal root ganglia after peripheral nerve lesions in the rat. Neuroscience 2002;112:23–38. [PubMed: 12044469]

Jessen KR, Mirsky R. Nonmyelin-forming Schwann cells coexpress surface proteins and intermediate filaments not found in myelin-forming cells: a study of Ran-2, A5E3 antigen and glial fibrillary acidic protein. Journal of Neurocytology 1984;13:923–934. [PubMed: 6398831]

Jessen KR, Thorpe R, Mirsky R. Molecular identity, distribution and heterogeneity of glial fibrillary acidic protein: an immunoblotting and immunohistochemical study of Schwann cells, satellite cells, enteric glia and astrocytes. Journal of Neurocytology 1984;13:187–200. [PubMed: 6726286]

Jimenez-Andrade JM, Peters CM, Mejia NA, Ghilardi JR, Mantyh PW. Sensory neurons and their supporting cells located in the trigeminal, thoracic and lumbar ganglia differentially express markers of injury following intravenous administration of paclitaxel in the rat. Neurosci Lett 2006;405:62–67. [PubMed: 16854522]

Jin SX, Zhuang ZY, Woolf CJ, Ji RR. p38 mitogen-activated protein kinase is activated after a spinal nerve ligation in spinal cord microglia and dorsal root ganglion neurons and contributes to the generation of neuropathic pain. J Neurosci 2003;23:4017–4022. [PubMed: 12764087]

Kajander KC, Sahara Y, Iadarola MJ, Bennett GJ. Dynorphin increases in the dorsal spinal cord in rats with a painful peripheral neuropathy. Peptides 1990;11:719–728. [PubMed: 1978300]

Kapadia SE, LaMotte CC. Deafferentation-induced alterations in the rat dorsal horn: I. Comparison of peripheral nerve injury vs. rhizotomy effects on presynaptic, postsynaptic, and glial processes. J Comp Neurol 1987;266:183–197. [PubMed: 2830320]

Krarup-Hansen A, Rietz B, Krarup C, Heydorn K, Rorth M, Schmalbruch H. Histology and platinum content of sensory ganglia and sural nerves in patients treated with cisplatin and carboplatin: an autopsy study. Neuropathol Appl Neurobiol 1999;25:29–40. [PubMed: 10194773]

Lee JJ, Swain SM. Peripheral neuropathy induced by microtubule-stabilizing agents. J Clin Oncol 2006;24:1633–1642. [PubMed: 16575015]

Lindholm D, Heumann R, Meyer M, Thoenen H. Interleukin-1 regulates synthesis of nerve growth factor in non-neuronal cells of rat sciatic nerve. Nature 1987;330:658–659. [PubMed: 3317065]

Ma W, Eisenach JC. Morphological and pharmacological evidence for the role of peripheral prostaglandins in the pathogenesis of neuropathic pain. Eur J Neurosci 2002;15:1037–1047. [PubMed: 11918652]

Ma W, Eisenach JC. Cyclooxygenase 2 in infiltrating inflammatory cells in injured nerve is universally up-regulated following various types of peripheral nerve injury. Neuroscience 2003;121:691–704. [PubMed: 14568029]

Mantyh PW. Cancer pain and its impact on diagnosis, survival and quality of life. Nat Rev Neurosci 2006;7:797–809. [PubMed: 16988655]

Meyer M, Matsuoka I, Wetmore C, Olson L, Thoenen H. Enhanced synthesis of brain-derived neurotrophic factor in the lesioned peripheral nerve: different mechanisms are responsible for the regulation of BDNF and NGF mRNA. J Cell Biol 1992;119:45–54. [PubMed: 1527172]

Mielke S, Sparreboom A, Mross K. Peripheral neuropathy: A persisting challenge in paclitaxel-based regimes. Eur J Cancer 2006;42:24–30. [PubMed: 16293411]

Molander C, G G. Spinal cord projections from hindlimb muscle nerves in the rat studied by transganglionic transport of horseradish peroxidase, wheat germ agglutinin congugated horseradish peroxidase, or horseradish peroxidase with dimethylsulfoxide. J Comp Neurol 1987;260:246–255. [PubMed: 3038969]

Mueller M, Leonhard C, Wacker K, Ringelstein EB, Okabe M, Hickey WF, Kiefer R. Macrophage response to peripheral nerve injury: the quantitative contribution of resident and hematogenous macrophages. Lab Invest 2003;83:175–185. [PubMed: 12594233]

Myers RR, Heckman HM, Rodriguez M. Reduced hyperalgesia in nerve-injured WLD mice: relationship to nerve fiber phagocytosis, axonal degeneration, and regeneration in normal mice. Exp Neurol 1996;141:94–101. [PubMed: 8797671]

Nichols ML, Lopez Y, Ossipov MH, Bian D, Porreca F. Enhancement of the antiallodynic and antinociceptive efficacy of spinal morphine by antisera to dynorphin A (1-13) or MK-801 in a nerve-ligation model of peripheral neuropathy. Pain 1997;69:317–322. [PubMed: 9085307]

Obata K, Yamanaka H, Fukuoka T, Yi D, Tokunaga A, Hashimoto N, Yoshikawa H, Noguchi K. Contribution of injured and uninjured dorsal root ganglion neurons to pain behavior and the changes in gene expression following chronic constriction injury of the sciatic nerve in rats. Pain 2003;101:65–77. [PubMed: 12507701]

Persohn E, Canta A, Schoepfer S, Traebert M, Mueller L, Gilardini A, Galbiati S, Nicolini G, Scuteri A, Lanzani F, Giussani G, Cavaletti G. Morphological and morphometric analysis of paclitaxel and docetaxel-induced peripheral neuropathy in rats. Eur J Cancer 2005;41:1460–1466. [PubMed: 15913989]

Peters CM, Ghilardi JR, Keyser CP, Kubota K, Lindsay TH, Luger NM, Mach DB, Schwei MJ, Sevcik MA, Mantyh PW. Tumor-induced injury of primary afferent sensory nerve fibers in bone cancer pain. Exp Neurol 2005;193:85–100. [PubMed: 15817267]

Peters CM, Jimenez-Andrade JM, Jonas BM, Sevcik MA, Koewler NJ, Ghilardi JR, Wong GY, Mantyh PW. Intravenous paclitaxel administration in the rat induces a peripheral sensory neuropathy characterized by macrophage infiltration and injury to sensory neurons and their supporting cells. Exp Neurol 2007;203:42–54. [PubMed: 17005179]

Pignata S, De Placido S, Biamonte R, Scambia G, Di Vagno G, Colucci G, Febbraro A, Marinaccio M, Lombardi AV, Manzione L, Carteni G, Nardi M, Danese S, Valerio MR, de Matteis A, Massidda B, Gasparini G, Di Maio M, Pisano C, Perrone F. Residual neurotoxicity in ovarian cancer patients in clinical remission after first-line chemotherapy with carboplatin and paclitaxel: the Multicenter Italian Trial in Ovarian cancer (MITO-4) retrospective study. BMC Cancer 2006;6:5. [PubMed: 16398939]

Postma TJ, Vermorken JB, Liefting AJ, Pinedo HM, Heimans JJ. Paclitaxel-induced neuropathy. Ann Oncol 1995;6:489–494. [PubMed: 7669713]

Quasthoff S, Hartung HP. Chemotherapy-induced peripheral neuropathy. J Neurol 2002;249:9–17. [PubMed: 11954874]

Rowinsky EK, Eisenhauer EA, Chaudhry V, Arbuck SG, Donehower RC. Clinical toxicities encountered with paclitaxel (Taxol). Semin Oncol 1993;20:1–15. [PubMed: 8102012]

Sahenk Z, Barohn R, New P, Mendell JR. Taxol neuropathy. Electrodiagnostic and sural nerve biopsy findings. Arch Neurol 1994;51:726–729. [PubMed: 7912506]

Scuteri A, Nicolini G, Miloso M, Bossi M, Cavaletti G, Windebank AJ, Tredici G. Paclitaxel toxicity in post-mitotic dorsal root ganglion (DRG) cells. Anticancer Res 2006;26:1065–1070. [PubMed: 16619507]

Seijffers R, Allchorne AJ, Woolf CJ. The transcription factor ATF-3 promotes neurite outgrowth. Mol Cell Neurosci 2006;32:143–154. [PubMed: 16713293]

Shinder V, Devor M. Structural basis of neuron-to-neuron cross-excitation in dorsal root ganglia. Journal of Neurocytology 1994;23:515–531. [PubMed: 7815085]

Shortland PJ, Baytug B, Krzyzanowska A, McMahon SB, Priestley JV, Averill S. ATF3 expression in L4 dorsal root ganglion neurons after L5 spinal nerve transection. Eur J Neurosci 2006;23:365–373. [PubMed: 16420444]

Stefansson K, Wollmann RL, Moore BW. Distribution of S-100 protein outside the central nervous system. Brain Res 1982;234:309–317. [PubMed: 7059833]

Stephenson JL, Byers MR. GFAP immunoreactivity in trigeminal ganglion satellite cells after tooth injury in rats. Exp Neurol 1995;131:11–22. [PubMed: 7895805]

Taniuchi M, Clark HB, Johnson EM Jr. Induction of nerve growth factor receptor in Schwann cells after axotomy. Proc Natl Acad Sci U S A 1986;83:4094–4098. [PubMed: 3012551]

Thomas, PK.; Landon, DN.; King, RHM. Diseases of the peripheral nervous system. Oxford University Press; New York: 1992.

Todd, AJ.; Koerber, HR. Neuroanatomical substrates of spinal nociception In Wall and Melzack's Textbook of Pain. 5. McMahon, SB.; Koltzenburg, M., editors. Elsevier; Philadelphia: 2006. p. 73-90.

Tofaris GK, Patterson PH, Jessen KR, Mirsky R. Denervated Schwann cells attract macrophages by secretion of leukemia inhibitory factor (LIF) and monocyte chemoattractant protein-1 in a process regulated by interleukin-6 and LIF. J Neurosci 2002;22:6696–6703. [PubMed: 12151548]

Tsuda M, Inoue K, Salter MW. Neuropathic pain and spinal microglia: a big problem from molecules in "small" glia. Trends Neurosci 2005;28:101–107. [PubMed: 15667933]

Tsuda M, Shigemoto-Mogami Y, Koizumi S, Mizokoshi A, Kohsaka S, Salter MW, Inoue K. P2X4 receptors induced in spinal microglia gate tactile allodynia after nerve injury. Nature 2003;424:778–783. [PubMed: 12917686]

Tsujino H, Kondo E, Fukuoka T, Dai Y, Tokunaga A, Miki K, Yonenobu K, Ochi T, Noguchi K. Activating transcription factor 3 (ATF3) induction by axotomy in sensory and motoneurons: A novel neuronal marker of nerve injury. Mol Cell Neurosci 2000;15:170–182. [PubMed: 10673325]

Tsuzuki K, Kondo E, Fukuoka T, Yi D, Tsujino H, Sakagami M, Noguchi K. Differential regulation of P2X(3) mRNA expression by peripheral nerve injury in intact and injured neurons in the rat sensory ganglia. Pain 2001;91:351–360. [PubMed: 11275393]

Wang MS, Davis AA, Culver DG, Wang Q, Powers JC, Glass JD. Calpain inhibition protects against Taxol-induced sensory neuropathy. Brain 2004;127:671–679. [PubMed: 14761904]

Wang R, Guo W, Ossipov MH, Vanderah TW, Porreca F, Lai J. Glial cell line-derived neurotrophic factor normalizes neurochemical changes in injured dorsal root ganglion neurons and prevents the expression of experimental neuropathic pain. Neuroscience 2003;121:815–824. [PubMed: 14568039]

Watkins LR, Milligan ED, Maier SF. Glial activation: a driving force for pathological pain. Trends in Neurosciences 2001;24:450–455. [PubMed: 11476884]Review

Woodham P, Anderson PN, Nadim W, Turmaine M. Satellite cells surrounding axotomised rat dorsal root ganglion cells increase expression of a GFAP-like protein. Neurosci Lett 1989;98:8–12. [PubMed: 2710403]

Xie WR, Deng H, Li H, Bowen TL, Strong JA, Zhang JM. Robust increase of cutaneous sensitivity, cytokine production and sympathetic sprouting in rats with localized inflammatory irritation of the spinal ganglia. Neuroscience 2006;142:809–822. [PubMed: 16887276]

Zhou XF, Deng YS, Chie E, Xue Q, Zhong JH, McLachlan EM, Rush RA, Xian CJ. Satellite-cell-derived nerve growth factor and neurotrophin-3 are involved in noradrenergic sprouting in the dorsal root ganglia following peripheral nerve injury in the rat. Eur J Neurosci 1999;11:1711–1722. [PubMed: 10215925]

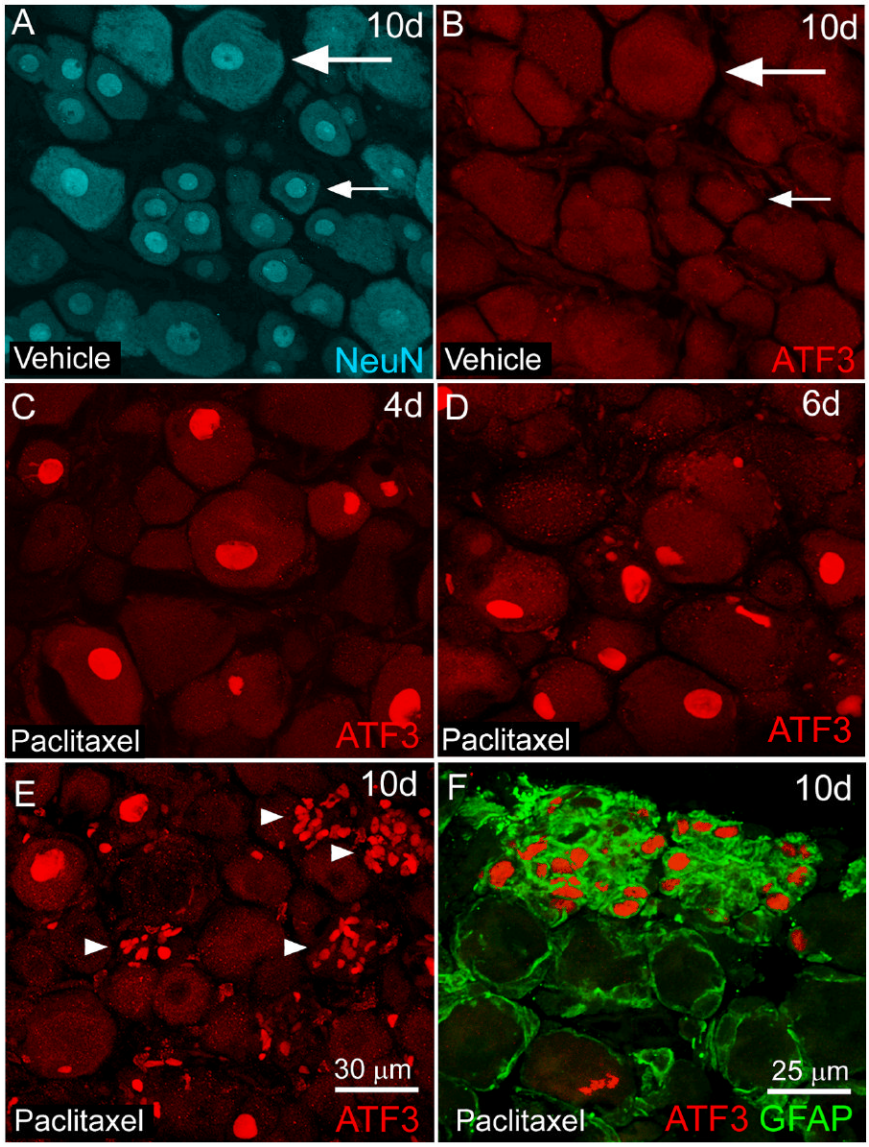

Figure 1.

Activating transcription factor 3 immunoreactivity (ATF3-IR) is increased in neurons and non-neuronal satellite cells in L4 dorsal root ganglia (DRG) of rats following intravenous paclitaxel administration. L4 DRG section from paclitaxel (C-F) and vehicle (cremephor/ethanol) treated rats (A,B) were examined immunohistochemically with antibodies against activating transcription factor (ATF3, red) a marker of cellular injury/regeneration at several time points following administration of paclitaxel. Sensory neurons in DRG were identified immunohistochemically with antibodies against NeuN (NeuN, blue) a neuronal nuclei marker (A) that labels both small (small arrow) and large (large arrow) diameter sensory neurons. Increased ATF3 immunoreactivity (IR) was observed in neuronal nuclei at day 4 (C) day 6 (D) and to a lesser extent at day 10 post paclitaxel administration (E). At day 10, there was also an increase in clusters of ATF3-IR satellite cells (E, arrowhead) within the DRG of paclitaxel-treated rats as these cells coexpressed the intermediate filament glial fibrillary acidic protein (F, GFAP, green). No ATF3 expression was observed in L4 DRG of vehicle-treated rats at day 10 (B) or other time points examined. Scale bar: A-E 30 μm. F: 25 μm.

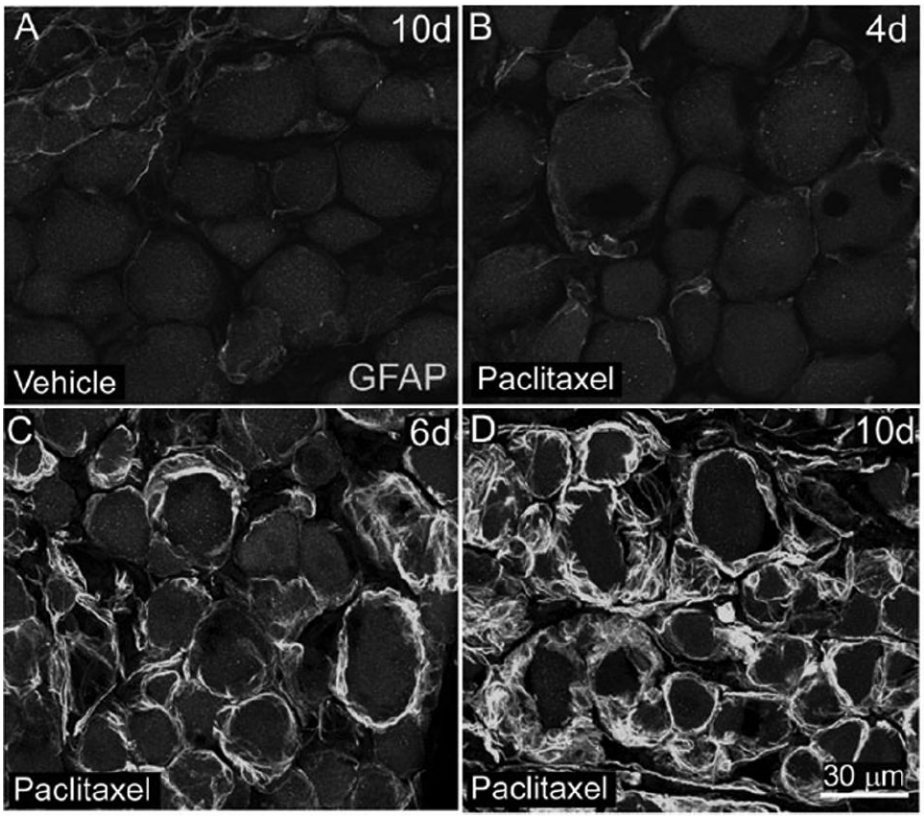

Figure 2.

Glial fibrillary acidic protein immunoreactivity (GFAP-IR) is increased in satellite cells surrounding sensory neurons in the L4 dorsal root ganglia (DRG) of rats following intravenous paclitaxel administration. L4 DRG sections from vehicle (cremephor/ethanol) (A) and paclitaxel-treated rats (B-D) were examined immunohistochemically with an antibody against GFAP, an intermediate filament present in DRG satellite cells. Increased GFAP-IR was observed at day 6 (C) and day 10 (D) following paclitaxel administration. DRG sections from paclitaxel treated rats at day 4 (B) or earlier time points displayed similar levels of GFAP-IR compared to vehicle-treated rats (A). Scale bars A-D = 30 μm.

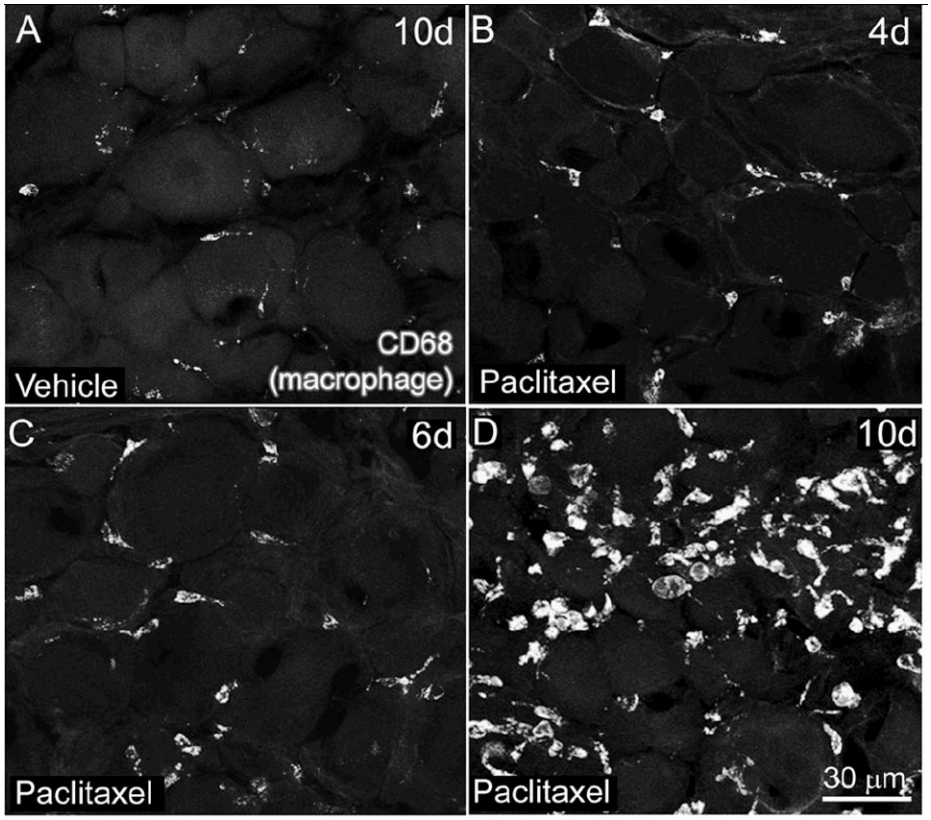

Figure 3.

The number of CD68 immunoreactive (IR) macrophages increased in L4 dorsal root ganglia (DRG) following intravenous paclitaxel administration. L4 DRG sections from vehicle (cremephor/ethanol) (A) and paclitaxel-treated rats (B-D) were examined immunohistochemically with an antibody against CD68 (clone ED1), an intracellular lysosomal protein that is expressed in activated macrophages. The number of CD68-IR macrophages increased in L4 DRG of paclitaxel treated rats beginning on day 6 through day 10. DRG sections from paclitaxel-treated rats day 4 (B) or earlier time points displayed similar numbers of CD68-IR macrophages compared to vehicle-treated rats (A). Note that CD68-IR macrophages in paclitaxel-treated rats were larger in size and formed aggregates around neuronal cell bodies (D). CD68-IR macrophages in vehicle-treated rats (C) were evenly dispersed throughout the DRG and were morphologically long and slender in appearance. Scale bars: A-D = 30 μm.

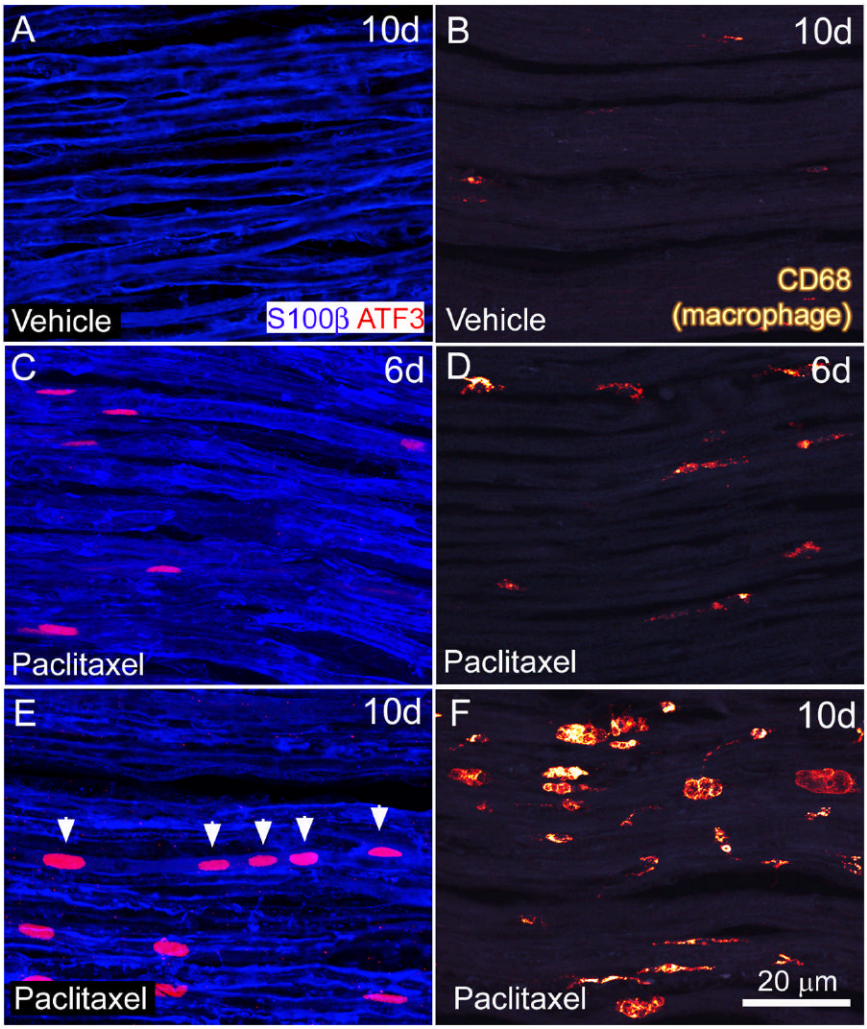

Figure 4.

Activating transcription factor 3 (ATF3) is upregulated in Schwann cells and the number of CD68-IR macrophages increases in the sciatic nerve of rats following paclitaxel administration. Sciatic nerve sections from midthigh level were immunohistochemically labeled with antibodies against S100β (blue) which labels the outermost portion of myelinating Schwann cells and ATF3 (red). The number of ATF3-IR S100β-IR within the sciatic nerve of paclitaxel-treated rats increased at day six (C) and day 10 (E) following paclitaxel administration compared to vehicle-treated rats (A). Note that Schwann cells expressing ATF-3 appeared to be grouped in a linear arrangement (arrowheads) as if a group of Schwann cells that ensheath the same injured axon upregulated ATF3. Similarly, the number and size of CD68-IR macrophages was greater in the sciatic nerve of paclitaxel-treated rats at day 10 (F) compared to vehicle-treated rats (B). The number of CD68-IR macrophages in the sciatic nerve of paclitaxel-treated rats at day 6 (D) and earlier time points was similar compared to vehicle-treated rats (B) Scale bars A-F = 20 μm.

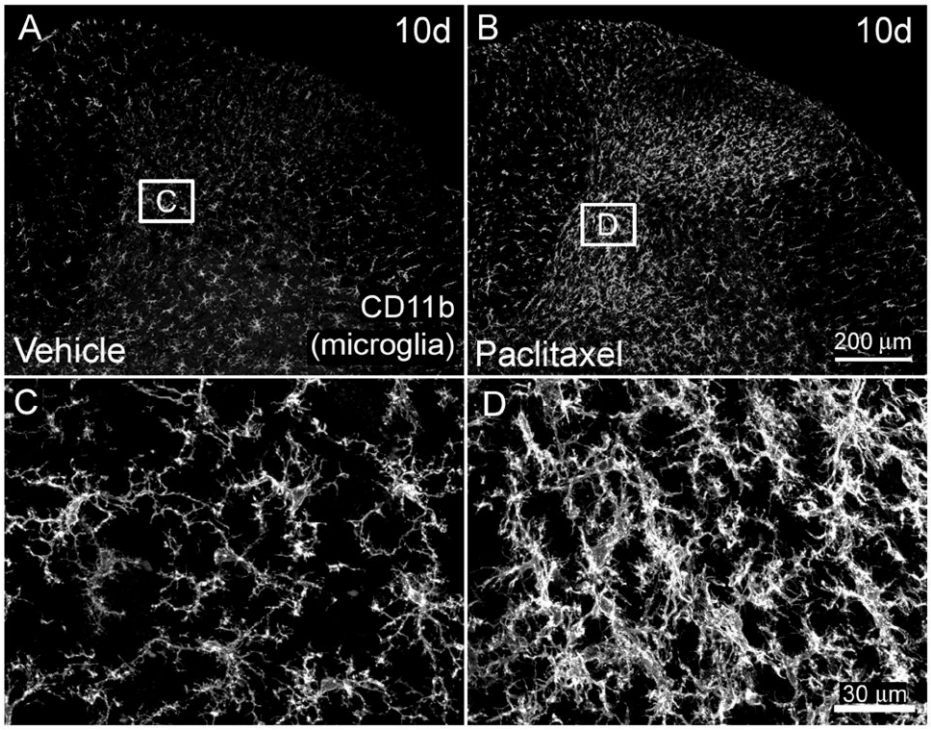

Figure 5.

CD11b immunoreactivity (CD11b-IR) is increased in microglia within the dorsal horn of the L4 spinal cord of paclitaxel-treated rats. Microglia in the spinal cord of vehicle (cremophor/ethanol) treated rats (A) are uniformly distributed throughout the gray matter. Beginning six and ten days (B) following initial intravenous administration of paclitaxel an increase in CD11b-IR microglia (CD11b) is present in the dorsal horn of the spinal cord (B). Note that the increased CD11b-IR is especially prominent in deeper laminae (III-VI) of paclitaxel-treated rats. Higher magnification shows increased density of microglia with hypertrophic morphology within the spinal cord of paclitaxel-treated rats (D), whereas microglia in vehicle-treated rats possess a more ramified appearance typical of resting microglia (C). Scale bar A, B = 200μm; C, D = 30μm.

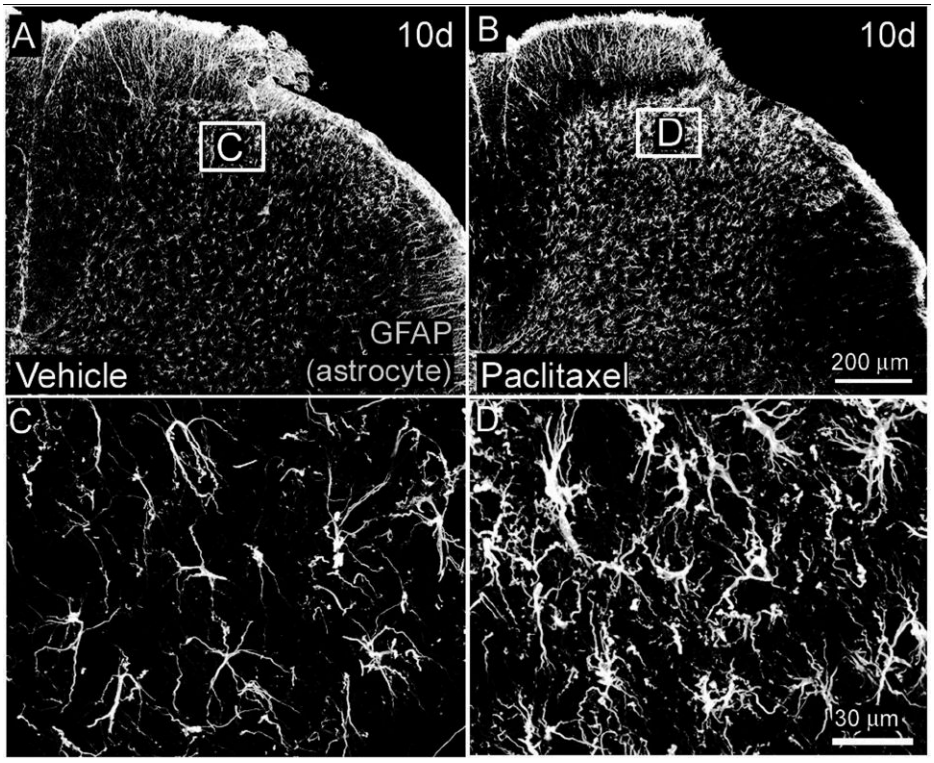

Figure 6.

Glial fibrillary acidic protein immunoreactivity (GFAP-IR) is increased in astrocytes within the L4 spinal cord of paclitaxel-treated rats. Beginning six and ten days (B) following intravenous administration of paclitaxel an increase in GFAP-IR is present in astrocytes throughout the dorsal horn (laminae I-VI) of the L4 spinal cord of paclitaxel-treated rats (B) compared to vehicle (cremophor/ethanol) treated rats (A). Higher magnification demonstrates that astrocytes in paclitaxel treated rats posses a more hypertrophic appearance typical of activated astrocytes (D) compared to vehicle-treated rats (C). Scale bar A, B = 200µm; C, D = 30µm.

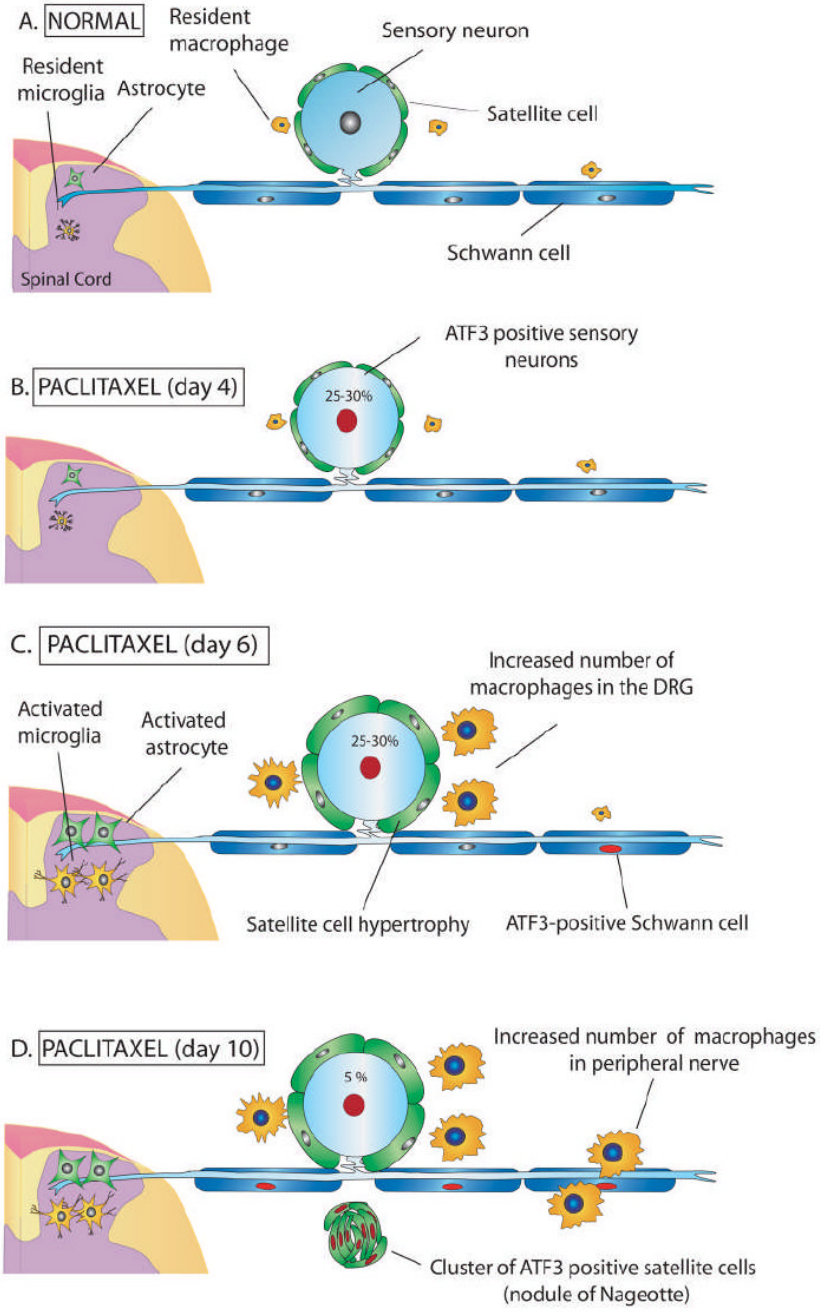

Figure 7.

Schematic diagram depicting a primary afferent neuron and supporting cells under normal conditions and following treatment with the chemotherapeutic agent paclitaxel. a) Normally sensory neuron cell bodies within the dorsal root ganglia (DRG) are surrounded by several satellite cells that maintain neuronal homeostasis by regulating extracellular ion concentrations and nutrient levels. Resident macrophages survey the local environment for signs of tissue injury or infection. Peripheral nerve axons are surrounded by Schwann cells and project to the spinal cord and peripheral tissues. Sequelae of cellular pathology occurs in the DRG, sciatic nerve, and spinal cord following repeat (Day 0 and 3) intravenous administration of paclitaxel. B) Four days post initial infusion a subset of DRG sensory neurons upregulate activating

transcription factor 3 (ATF3, red nuclei) and exhibit displaced nuclei indicative of an injured phenotype. C) Six days post initial infusion there is activation of DRG satellite cells evident as hypertrophy and increased immunoreactivity for glial fibrillary acidic protein (GFAP) as well as an increase in the number of activated (CD68-IR) macrophages in the DRG. Both microglial and astrocyte activation is present in the spinal cord beginning six days post initial infusion. D) Ten days post initial infusion nodules of Nageotte form in the DRG evident as clusters of ATF3-IR satellite cells. This feature has been suggested to indicate degeneration and loss of neuronal cell bodies. The number of CD68-IR macrophages and the expression of ATF3 in Schwann cells is increased within the sciatic nerve at day 10. Collectively, these changes in the DRG, peripheral nerves and spinal cord may be involved in the positive painful symptoms such as pain, cold allodynia, and myalgias seen in patients treated with paclitaxel as well as sensory deficits including loss of two-point discrimination, vibratory sense, and proprioceptive abilities.

Table 1

Evolving cellular pathology in dorsal root ganglia (L4), sciatic nerve and spinal cord following intravenous paclitaxel in the rat

Summary of quantification of cellular changes in paclitaxel-treated rats compared to values obtained from vehicle-treated rats at the same time point. For immunofluorescence measurements results are as follows: Horizontal arrows no significant change, one arrow 100-200% increase, two arrows 200-300% increase, three arrows 300-400 % increase, four arrows more than 500% increase compared to relative vehicle values. For counts of neuronal ATF3 expression in the DRG, low or null levels in vehicle-treated rats made calculating fold increase from vehicle values difficult. Therefore, arrows indicate actual values as percentage of total neurons labeled in L4 ganglia of paclitaxel treated rats. Horizontal arrows no significant ATF3 expression, one arrow 1-5%, two arrows 5-10%, three arrows 10-20%, and four arrows greater than 20% (complete values for experimental and control rats are in text).

	Time post-injection			
	Day 1	**Day 4**	**Day 6**	**Day 10**
DRG				
Neurons (ATF3, %)	↗	↗↗↗↗	↗↗↗↗	↗↗
Satellite cells (GFAP, IF)	↔	↔	↗↗↗↗	↗↗↗↗
Macrophages (CD68, #)	↔	↔	↗↗	↗↗↗↗
Nodule of Nagoette (GFAP/ATF3, #)	↔	↔	↔	↗↗↗↗
Sciatic nerve				
Schwann cell (GFAP, IF)	↔	↔	↔	↔
Schwann cell (S100β/ATF3, #)	↔	↔	↗	↗↗
Macrophages (CD68, #)	↔	↔	↔	↗↗↗↗
Spinal cord				
Astrocyte (GFAP, IF)				
Laminae I-II	↔	↔	↗	↗
Laminae III-VI	↔	↔	↗	↗
Microglia (CD11b, IF)				
Laminae I-II	↔	↔	↔	↔
Laminae III-VI	↔	↔	↗	↗↗↗
Neurons (ATF3, #)	↔	↔	↔	↔